

Figure 2 below shows a more detailed, engineering schematic of the cook stove design chosen. An air inlet at the bottom of the stove allows fresh air to be sucked through the grate and fuel bed. High temperatures in the fuel bed heat the air and cause pyrolysis. The gasses emitted from the fuel undergo combustion with air in the combustion chamber. The heat generated from combustion further heats up the hot gasses as well as providing energy for further pyrolysis of fuel, sustaining the combustion reaction. At this point, the hot gasses speed up as they pass through a nozzle and impinge upon a pot, heating it up. These gasses are redirected around the sides of the pot by a skirt through a channel gap, where they further contribute to heat transfer to the pot.

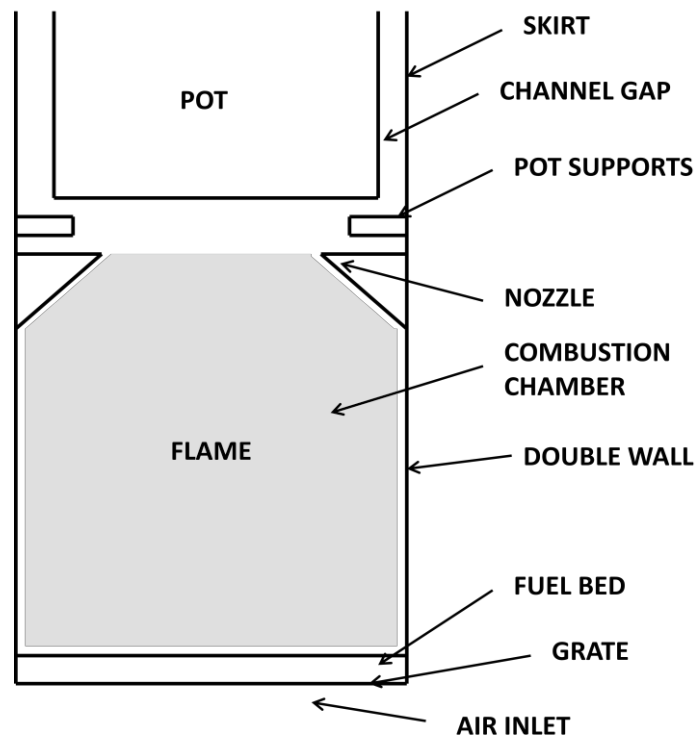


Figure 2. Engineering schematic of a cookstove

Figure 2 depicts the design that Open Hearth Surgery has chosen to analyze and optimize throughout the course of the design process. Essentially, it is consistent with the design of a Rocket Stove, which has already been proven more efficient than the three stone fire (described in Appendix B). However, the innovation lies within the unique combination of the aforementioned nozzle, and the skirt surrounding the pot. The implementation of these two design elements poses an interesting coupling of the thermophysical properties present within the cook stove, and will be analyzed to meet the design objective and criteria mentioned above.

APPROACH

The primary goal of this design is to explore how variations in the team's unique cook stove geometry influence efficiencies, emissions, and cost. Because cost is primarily dependent on material and manufacturing factors, it can be reduced by using inexpensive materials and utilizing a simple design. Clever business models, as described in previous sections and in the

Appendices, also help lower cost so that efficient cook stoves can be available to anyone [6]. Emissions are difficult to model due to the complex chemical reactions that go on during combustion. As a result, the best way to approach this portion of the objective is a generalized approach that takes into account certain standards and rules of thumb of cook stove design that have been experimentally determined. This includes utilizing certain height to diameter ratios of the combustion chamber and burning fuel lean so as to reduce CO emissions. This leaves only one primary goal that can be readily quantified and optimized: efficiency. This became apparent early in the design process. The primary areas of focus should be the interaction of fluid flow, heat transfer, and combustion within the stove.

These theoretical areas of focus are highly coupled within a cook stove. They all are dependent upon one another. In fact, Kausley gives a theoretical relation that relates the fuel to air ratio with the flame temperature [7]. For any set fuel to air ratio, a certain flame temperature should result. This is very convenient and allows the complex combustion processes to be neglected. Instead, a certain flame temperature, set to be equal to the incoming air temperature, is assumed. With a known temperature of incoming air, relationships for fluid flow, heat transfer, and eventually, efficiency can be quantified and determined. This allows the optimization of a stove with varying geometrical parameters.

Inputs

The primary inputs into the stove system can be either variable or constant. Variable inputs are the geometries that are parameterized. By selecting a variety of geometrical parameters in a reasonable range for cook stoves, dimensions that yield optimum results can be selected for final design. Constants chosen are based on general knowledge and measured values common in most stoves. They do not vary across different stove designs.

The inputs shown in Table 1 below are variable and parameterized later in the optimization.

Table 1. Input Variables

<i>Input Designation</i>	<i>Description</i>	<i>Units</i>	<i>Lower Bound</i>	<i>Upper Bound</i>
D_n	Nozzle Diameter	cm	20 cm	40 cm
G_s	Gap between pot wall and stove wall	mm	2 mm	12 mm
H	Height of pot	cm	20 cm	40 cm
D_p	Diameter of pot	cm	20 cm	40 cm

The inputs in Table 2 are those which are chosen based on available literature, general recommendations for stove design, and common knowledge.

Table 2. Chosen Inputs and Values

<i>Input Designation</i>	<i>Description</i>	<i>Units</i>	<i>Chosen Value</i>
T_f	Flame Temperature	K	860 K [7]
T_b	Bed Temperature	K	650 K [7]
T_w	Water Temperature	K	373.15 K

Control Volume Analysis

The primary geometry that is intended to be explored concerns the relationship between efficiency of a cook stove and changing nozzle diameter and skirt gap. Changing these parameters affects fluid flow, convective and radiative heat transfer, and efficiency. Other geometric relations to be explored include the effects of changing skirt length and stove diameter. Finding out how variations in these parameters affect the stove as well as their relative importance in stove performance should lead to better stove designs.

Parameterizing key variables to stove performance will allow equations and models to be created. This cannot be done by looking at the system as a whole but will instead be done by splitting up the stove into multiple control volumes and utilizing an energy balance on each control volume. This yields a system of equations that can be optimized and solved. Figure 3 below depicts the control volumes used to analyze the stove.

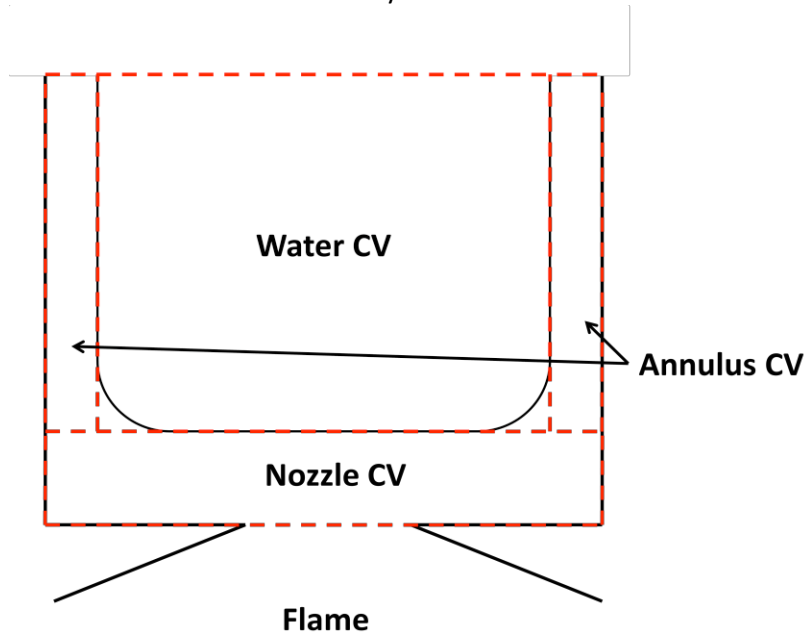


Figure 3. Control Volumes within the Stove

A couple of assumptions have been made for the generalized stove system. One major assumption is that the flame fills the entire volume of the combustion chamber. This is a reasonable assumption stoves are often designed with an approximate height to diameter ratio within the combustion chamber of 3:1. A larger combustion chamber allows for a larger flame, giving more time for all the fuel and volatiles to be burnt to completion [5]. This reduces emissions and increases efficiency. But even more importantly, it implies that the combustion process takes place throughout the combustion chamber. If combustion takes place within the entire chamber, then the flame also fills the entire chamber. By making this assumption, it is possible to look up a literature value for the temperature of the flame, and thereby the inlet temperature of the hot flue gasses into the nozzle area.

Another assumption made in the overall model is that the double wall of the stove is considered adiabatic. It is commonly recommended to use sheet metal to make stoves due to its low thermal mass [5]. But it is still important to insulate the stove and reduce losses through its walls. As a result, a double wall made of sheet metal is chosen. The double wall, when made of a low emissivity material, serves as a radiation shield to prevent radiation heat transfer from

the bed and the flames to the environment. Polished stainless steel is chosen as the material because its emissivity is approximately .20 between 400 and 800K [10]. By placing a small gap in between the two metal walls, the air within can be treated as a static insulator because there is very little advection present. As a result, conduction within the fluid dominates. Air is a very good insulator with a fluid conductivity value of .03 W/mK. Glass fiber insulation has a conductivity value around .04 W/mK, depending on its density [10]. The walls of the stove are well insulated. Assuming adiabatic wall conditions is a very reasonable simplifying assumption that makes the problem much simpler to work with.

Outputs

Beginning with inputs we can apply control volume analyses, simplifying assumptions, and constraint equations. From these, useful outputs that help understand the stove system can be realized. The useful outputs that lend insight into the performance of the stove system are presented in Table 3 below.

Table 3. Output Variables

Variable	Description	Units
$q_{conv,s}$	Convective heat transfer to pot bottom	W
$q_{conv,ps}$	Convective heat transfer to pot sides	W
q_{rad}	Radiative heat transfer to pot bottom	W
q_{tot}	Total heat transfer to pot	W

Even so, the primary output that should be maximized is the efficiency of the stove system, presented in Table 4. A higher efficiency stove ultimately creates the least waste. A high efficiency stove requires less fuel for a set task than a less efficient stove. This leads to less time spent gathering fuel as well as the conservation of vegetation in the surrounding environment. This is also reflected in emissions because less fuel is burned, therefore less particulate and chemical pollution is emitted. Efficiency is commonly defined as the ratio of useful work over the total amount of work done. In the case of a cook stove, that can be translated to be the total heat transfer to the pot's contents over the total amount of energy released.

Table 4. Stove Efficiency Output

Variable	Description	Units
η	Stove Efficiency	dimensionless

EQUATIONS

Geometric Relations

The design of the stove focuses on the alteration of geometries to optimize efficiency. These geometries are shown in Figure 4, below. The dimensions of the skirt and nozzle were altered over a range and the heat transfer to the pot found. Due to the nature of the stove some of the dimensions are unique to the design. The flow goes vertically from the bottom to the top. After flowing through the nozzle the flow will be radial until the annulus.

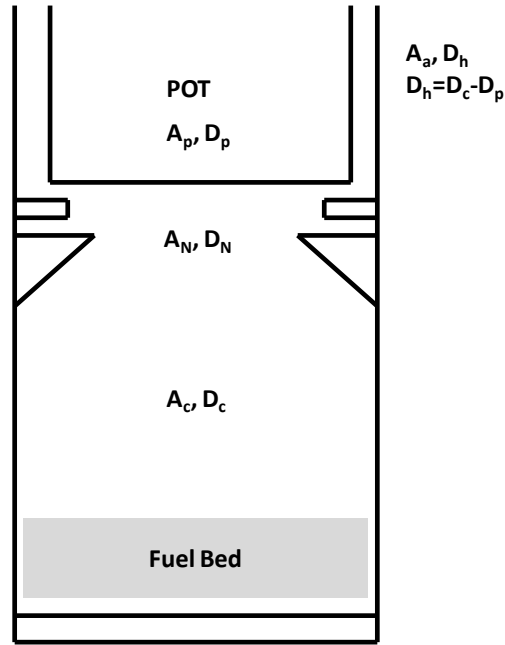


Figure 4. Areas and Diameters within a Stove

The area between the nozzle and the bottom of the pot is designed to maintain a constant velocity. To accomplish this, a continuity equation can be used and the gap is found to be inversely related to the diameter of the pot, as shown in Equation 6.

$$G_p = \frac{A_a}{\pi D_p} \quad (\text{Eq. 6})$$

Another important aspect is the annulus, as associated with the skirt of the pot. The several equations use values based on the dimensions of the annulus. An important value is the hydraulic diameter. Equation 7 shows the process of solving for the hydraulic diameter.

$$D_h = \frac{4A}{P} = \frac{4(.25)\pi(D_c^2 - D_p^2)}{\pi(D_c - D_p)} = D_c - D_p \quad (\text{Eq. 7})$$

The hydraulic diameter is a ratio of the cross sectional area, A , of the flow and the wetted perimeter, P . The solution shows that the hydraulic diameter is just the difference between the outer and inner diameters of the annulus.

Air Properties

Equations governing the fluid flow, heat transfer, and thermodynamic aspects of a cook stove are often dependent upon the thermophysical properties of the working fluid. Although these properties can easily be found in reference tables, they vary with respect to temperature. As a result, it is not realistic to constantly look up these values by hand. In order to avoid this, lines of best fit can be calculated for these values. Equations 8-13 represent the following curve fits for specific thermodynamic properties of air calculated for temperatures ranging from 300K to 1600K. Data has been gathered from Table B-2 of *SFPE Handbook of Fire Protection Engineering* [11] as well as Appendix A of *Fundamentals of Heat and Mass Transfer* [10] for density, specific heat, viscosity, kinematic viscosity, conductivity, and diffusivity of air. They most

always yield errors of less than 1%. A sample calculation of this method is detailed in Appendix E of this report.

$$\text{Density} = \rho(T) = 360.77819 * T^{-1.00336} \quad (\text{Eq. 8})$$

$$\begin{aligned} \text{Specific Heat} = C_p(T) = & 1.9327 * 10^{-10}T^4 - 7.9999 * 10^{-7}T^3 + \\ & 1.1407 * 10^{-3}T^2 - 4.4890 * 10^{-1}T + 1.0575 * 10^3 \end{aligned} \quad (\text{Eq.9})$$

$$\begin{aligned} \text{Viscosity} = \mu(T) \\ = 5.2880 * 10^{-14}T^3 - 7.5906 * 10^{-11}T^2 + 8.1485 * 10^{08}T - 4.4591 * 10^{-7} \end{aligned} \quad (\text{Eq. 10})$$

$$\begin{aligned} \text{Kinematic Viscosity} = \nu(T) \\ = -1.1555 * 10^{-14}T^3 + 9.5728 * 10^{-11}T^2 + 3.7604810^{-8}T - 3.4484 * 10^{-6} \end{aligned} \quad (\text{Eq. 11})$$

$$\begin{aligned} \text{Conductivity} = k(T) \\ = 1.5207 * 10^{-11}T^3 - 4.8574 * 10^{-8}T^2 + 1.0184 * 10^{-4}T - 3.9333 * 10^{-4} \end{aligned} \quad (\text{Eq. 12})$$

$$\text{Diffusivity} = \alpha(T) = 9.1018 * 10^{-11}T^2 + 8.8197 * 10^{-8}T - 1.0654 * 10^{-5} \quad (\text{Eq. 13})$$

The working fluid throughout the stove is approximated to be air. In reality, the flue gasses flowing through a stove have a different chemical composition than air. However, when running fuel lean so that CO emissions are reduced, the differences in the properties of air and flue gas become negligible. The gas composition of flue gasses for an excess air ratio of 162% is given by Kausley [7]. The calculation of flue gas density using partial pressures yields less than 1% error from tables giving the density of air. This calculation is detailed in Appendix E. Treating flue gasses as a gas with the same properties of air also is found in existing literature. Steward assumes that heat capacities of air, combustion products and fuel to be equal and independent of temperature in his paper on the height of buoyant diffusion flames [8].

Fluid Flow

Fluid flow in the stove is governed by a few equations: Bernoulli's, continuity, and momentum. Figure 5 illustrates fluid gas flow throughout the stove design as well as the important variables associated with the velocities at key points within the flow. By observing properties of the air, as reported above, and gases at points in the stove, relations can be determined. In most cases the temperature of the air or gas determines density or pressure.

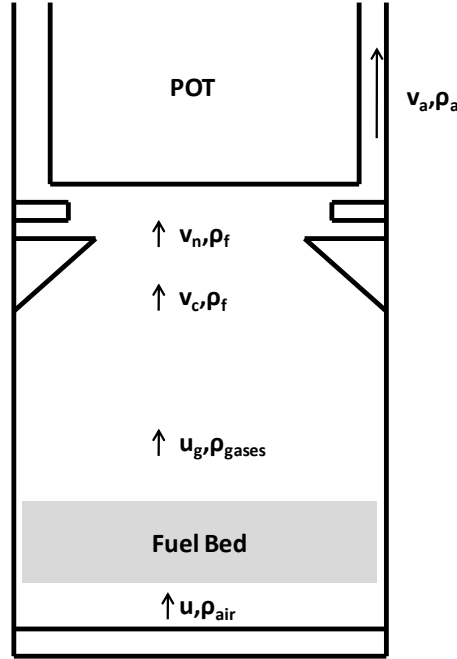


Figure 5. Velocities and Densities within a Stove

Equation 14 is the foremost equation for finding the flow rate: Bernoulli's equation.

$$\frac{\Delta p_1}{g\rho_1} + \frac{v_1^2}{2g} + H_1 = \frac{\Delta p_2}{g\rho_2} + \frac{v_2^2}{2g} + H_2 + \text{losses} \quad (\text{Eq. 14})$$

Simplifying Equation 14 with the considerations applicable to the stove yields Equation 15 and Equation 16 below. This is almost identical to an equation for Stove Suction used by Kausley [7].

$$\frac{1}{2}\rho_{air}u_i^2 = gH(\rho_{air} - \rho_{gases}) - \sum \Delta P \quad (\text{Eq. 15})$$

Coefficients Y and Z are introduced so that the entire fluid flow system can be represented by constants multiplied by the inlet fluid flow velocity, u_i .

$$Yu_i^2 = Z - \sum \Delta P \quad (\text{Eq. 16})$$

The unknowns are the inlet velocity and the sum of the pressure drops. Pressure drops occur throughout the stove and are result of several phenomena. These pressure drops include pipe flow, flow through a packed bed, and flow through changes in geometry. Each pressure drop equation uses additional fluid laws to get common variables.

First, Equations 17 and 18 address the pressure drop from flow through a packed bed. Equation 17 is a function of the velocity. It is further simplified by setting coefficients A and B to the coefficients of u_i , similar to the previous simplifications. This is shown in Equation 18.

$$\Delta P_{bed} = \frac{150\mu_b(1-\varepsilon)^2H_b}{d_p^2\varepsilon^3\phi^2}u_i + 1.75\frac{\rho_b(1-\varepsilon)H_b}{d_p\varepsilon^3\phi}u_i^2 \quad (\text{Eq. 17})$$

$$\Delta P_{bed} = Au_i + Bu_i^2 \quad (\text{Eq. 18})$$

Next, flow through the skirt is considered. This flow uses an adapted version of common pipe flow pressure drop, modeled by Equation 19.

$$\Delta P_{duct} = f \left(\frac{L}{D} \right) \left(\frac{u_a^2}{2} \right) \rho_a \quad (\text{Eq. 19})$$

Because the skirt and pot system creates an annulus for the gases to flow through, the application requires some variable alteration. The diameter of a pipe becomes the D_h , the hydraulic diameter. Using continuity, the velocity in the annulus can be found to have a ratio to the inlet velocity. This value is substituted to gain a common variable, as shown in the progression from Equation 20 to 21.

$$\Delta P_{annulus} = f \left(\frac{L}{D_h} \right) \left(\frac{\rho_a}{2} \right) \left(\frac{\rho_{air} A_b}{\rho_a A_a} \right)^2 u_i^2 \quad (\text{Eq. 20})$$

$$\Delta P_{annulus} = C u_i^2 \quad (\text{Eq. 21})$$

The nozzle of the stove also accounts for pressure drops. In order to model the nozzle, the flow was assumed to suddenly go from a large pipe to a small pipe then from a small pipe to a large pipe. Because of the nearly instantaneous nature of this model, the pressure drop is an over estimation of the pressure drop associated with the stove nozzle. Equations 22 and 23 model this flow, which is based on ratios of the diameters of the two pipes.

$$\Delta P_{nozzle,1} = \frac{\rho_f}{2} \left[\left(\frac{\rho_{air} A_b}{\rho_f A_n} \right)^2 + \left(\frac{\rho_{air} A_b}{\rho_f A_c} \right)^2 \right] u_i^2 = D u_i^2 \quad (\text{Eq. 22})$$

$$\Delta P_{nozzle,2} = u_i^2 \frac{1}{2} \left(\frac{\rho_{air} A_b}{\rho_f A_n} \right)^2 \rho_f \left[1 - \frac{D_n^2}{D_c^2} \right]^2 = E u_i^2 \quad (\text{Eq. 23})$$

Equation 22 is originally a function of the velocity for the large and small diameter pipe. The two velocities can be put in terms of the inlet velocity through continuity. Equation 23, the second nozzle equation, is originally based on the velocity of the small pipe and the diameters of the two pipes. Again, continuity is used to generate an equation in terms of the inlet velocity.

Now, the simplified Bernoulli's equation can be rearranged to sum the different portions to zero. Next the different pressure drops must be added to get the final equation for finding velocity, as shown in Equations 24 and 25.

$$Y u_i^2 + \sum \Delta P - Z = 0 \quad (\text{Eq. 24})$$

$$[Y + B + C + D + E] u_i^2 + A u_i - Z = 0 \quad (\text{Eq. 25})$$

Subsequently, Equation 25 is in the quadratic form, providing the ability to solve for the inlet air velocity, u_i .

Throughout the fluid equations continuity is used to get common variables. Equation 26 balances to give Equation 27, which is equivalent to the desired velocity.

$$u_a A_a \rho_a = u_b A_b \rho_b \quad (\text{Eq. 26})$$

$$u_a = \frac{u_b A_b \rho_b}{A_a \rho_a} \quad (\text{Eq. 27})$$

The velocity, cross sectional area, and density are used in the calculation of velocities. Once temperatures are determined the geometry is used to find the velocity anywhere in the stove.

Heat Transfer

Figure 6 below shows the Temperatures and Heat Transfer with a Stove. There are six unknown temperatures: T_n , T_a , T_{anv} , T_e , T_{p1} , and T_{p2} . The temperature of the flame, T_f , is given as 860K for actual flame temperature when 162% excess air available [7]. Bed temperature, T_b , can be set to 650K for wood undergoing pyrolysis [7]. Furthermore, the water can be assumed to be at boiling temperature. It is common knowledge that the temperature of boiling water is 100°C, or 373.15K. Ambient air temperature can be assumed to be 20°C, or 293.15K. The two mechanisms of heat transfer that are present in the diagram are radiation, which occurs from the fuel bed to the bottom of the pot, and convection, which occurs around all the surfaces of the pot. Heat losses through the exterior stove walls can be neglected due to adiabatic surface assumptions. The unknown temperatures are solved for primarily in two ways. Expressions can be set up relating the temperature drop of the fluid to the heat transfer from the fluid. Also, due to steady state conditions and assumptions, heat transfer rates into and out of pot surfaces can be made equivalent.

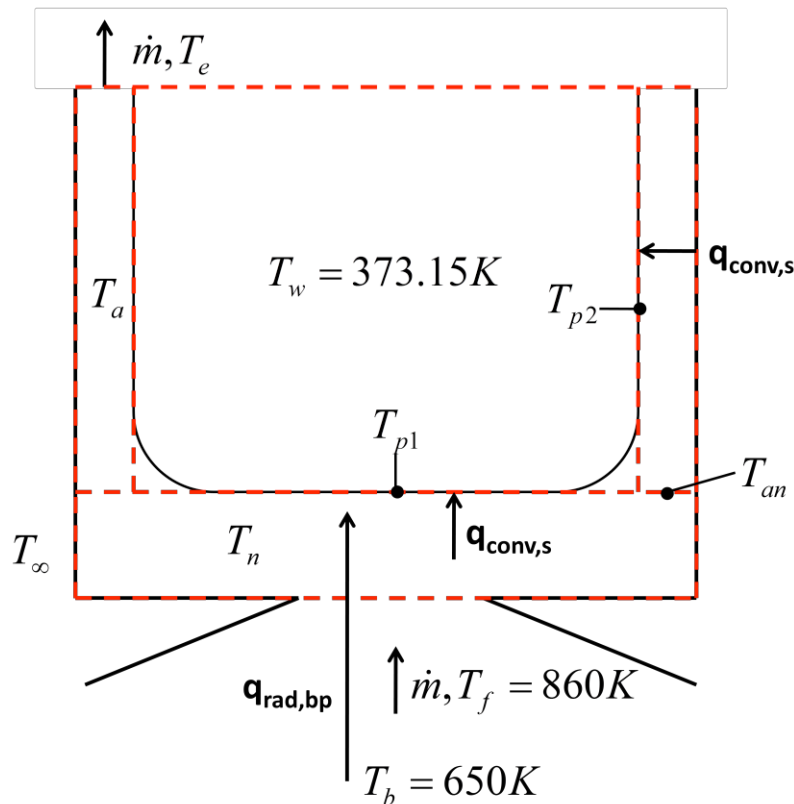


Figure 6. Temperatures and Heat Transfer within a Stove

In control volume analysis, it is customary to use average temperatures. Steward makes such an assumption in his paper as well [8]. Applying this to the specific circumstances depicted above, we find that the average temperature within the nozzle control volume is equal to the average of the inlet and outlet temperatures. Likewise, the average temperature within the

annulus control volume is equal to the average of the inlet and outlet temperatures. This gives the following relations of Equation 28 and 29.

$$T_n = \frac{T_{an} + T_f}{2} \quad (\text{Eq. 28})$$

$$T_a = \frac{T_{an} + T_e}{2} \quad (\text{Eq. 29})$$

Radiation

Radiation Heat Transfer is considered to occur solely from the fuel bed of the stove to the pot. The effect of flame radiation is neglected. Steward makes this assumption [8], and Hottel shows that flame emissivity is quite low and only around 7% [12]. Even so, radiation from the fuel bed to the pot should be considered. Because the bottom of the pot is directly exposed to flames, it is expected to be highly sooted. Its surface can be considered to act as a blackbody with an emissivity of unity [4]. Vegetation has an emissivity between .92 and .96 [10]. Because the fuel for this stove is wood or biomass, the fuel bed is considered to have an emissivity of .94. Equation 30 is used for radiation from the fuel bed to the pot.

$$q_{rad,bp} = \sigma \varepsilon_b F_{bp} A_b (T_b^4 - T_{p1}^4) \quad (\text{Eq. 30})$$

As the nozzle diameter changes, the view factor from the fuel bed to the pot will change as well. It is assumed that the nozzle has a smaller diameter than the pot and that it is located close to the pot to increase convective heat transfer. Because the nozzle is made out of the same material as the stove walls, it has been chosen to have a low emissivity. The emissivity for polished stainless steel is approximately .20 between 400 and 800 K [10]. This means a smaller nozzle shields the pot from radiation. As a result, the view factor from the fuel bed to the pot is defined as all the radiation that is emitted from the fuel bed and passes through the nozzle. The view factor from the fuel bed to the pot, F_{bp} , can be calculated utilizing the view factor for coaxial parallel disks, detailed in Equations 31-34 [10]. Consider the disks represented by the fuel bed and nozzle. Their respective radii are $D_b/2$ and $D_n/2$. They are separated by a distance of H , the height of the combustion chamber. R is a characteristic radius and S is a simplifying variable.

$$R_n = D_n/2H \quad (\text{Eq. 31})$$

$$R_b = D_b/2H \quad (\text{Eq. 32})$$

$$S = 1 + \frac{1+R_n^2}{R_b^2} \quad (\text{Eq. 33})$$

$$F_{bp} = \frac{1}{2} \left\{ S - \left[S^2 - 4 \left(\frac{D_n}{D_b} \right)^2 \right]^{\frac{1}{2}} \right\} \quad (\text{Eq. 34})$$

Convection at Pot Bottom

Impingement of a gas traveling through a single circular nozzle where the nozzle is located within one nozzle diameter from the surface is examined by Lytle and Webb [15]. The closeness of a nozzle to a surface is described as the ratio of the nozzle diameter to nozzle plate spacing, z/D_n . It can be generally stated that for a nozzle located closer to the impinging plate, or small z/D_n , the average heat transfer coefficient increases. However, for ratios of $z/D_n < .25$, significant acceleration of the fluid must occur between the nozzle-plate gap. As a result, a ratio of z/D_n equal to .25 is chosen so as not to invalidate the pressure drop equations previously described. They give the following empirical expression, Equation 35, for average Nusselt numbers over a plate radius approximately equal to nozzle diameter.

$$Nu_{D_n} = .424Re_{D_n}^{.57} \left(\frac{z}{D_n}\right)^{-.33} \quad (\text{Eq. 35})$$

The expression is valid for the range of nozzle-plate spacings of $.1 < z/D_n < 1$ and Reynolds numbers between 3600 and 27600. It has an average error of 9%. The average convective heat transfer coefficient can be found using Equation 36.

$$Nu_{D_n} = \frac{h_s D_n}{k_{air}} \quad (\text{Eq. 36})$$

Once this value is known, convective heat transfer to the bottom of the pot can be calculated using Equation 37.

$$q_{conv,s} = h_s A_s (T_n - T_{p1}) \quad (\text{Eq. 37})$$

Convection in Skirt

Jaco Dirker and Josua Meyer have compiled a list of popular equations describing the Nusselt number in a smooth annulus during forced convection [13]. They also have affirmed these equations, via experimentation and examination of previous literature, and recommended that the McAdams or Dittus-Boelter equations be used for annuli with annular diameter ratios of less than 2.5. McAdams describes the Nusselt Number as shown in Equation 38.

$$Nu_{Dh} = .023Re_{Dh}^8 Pr^{1/3} \left(\frac{\mu_{air}}{\mu_w}\right)^{.14} \quad (\text{Eq. 38})$$

Although this expression is for fully developed flow, the entrance region effects can be neglected due to the low velocity of flow and the narrow entrance region of the annulus [4]. The average convective heat transfer coefficient can be found using Equation 39.

$$Nu_{Dh} = \frac{h_a D_p}{k_{air}} \quad (\text{Eq. 39})$$

These equations, along with the respective values for viscosity, conductivity of a fluid, and geometrical constraints, yield Equation 40, an expression for the average heat transfer coefficient within the skirt section of the pot.

$$q_{conv,a} = h_a A_{ps} (T_a - T_{p2}) \quad (\text{Eq. 40})$$

Convection within Pot

The primary goal of a stove is not to heat up the pot, but actually to heat up the contents of the pot. As a result, the convection from the pot to the water must be considered. Because the pot is made of a high conductivity material, thermal resistance within the pot itself is neglected. It is assumed that a stove will most often be operating with liquid inside the stove at boiling temperature. Boiling occurs in multiple regimes: free convection boiling, nucleate boiling, transition boiling, and film boiling [10]. A pot with visible boiling water and bubbles that form at a hot surface and then rise is categorized under the nucleate boiling regime. The average convection coefficient for boiling water in nucleate boiling is experimentally approximated by Fritz in Equation 41[14].

$$\frac{h_w}{W/m^2K} = 1.95 \left(\frac{q_{conv,s}}{\frac{A}{W}} \right)^{.72} \quad (\text{Eq. 41})$$

This approximation holds at approximately one atmosphere of pressure and under the conditions

$$10^4 \frac{W}{m^2} < \frac{q_{conv,s}}{A_s} < 10^6 W/m^2$$

Although boiling mechanisms have been studied extensively, complete and reliable mathematical models have yet to be developed [10]. As a result, a first order approximation is used to find a conservative value of 2500 W/m²K for the convection coefficient between the pot and the water. The details of this analysis are contained in Appendix F.

With this assumption made, we can further describe heat transfer from the pot bottom to the water can with Equation 42.

$$q_{conv,p1} = h_w A_s (T_{p1} - T_w) \quad (\text{Eq. 42})$$

Furthermore, heat transfer from the pot side to the water can be described by Equation 43.

$$q_{conv,p2} = h_w A_{ps} (T_{p2} - T_w) \quad (\text{Eq. 43})$$

Heat Loss through the Stove

Although all of these equations and relations can readily yield expressions for heat transfer, they assume that the temperatures are known. However, that is not the case. It is necessary to develop a system of equations relating the temperatures present in the stove with the heat transfer various sections of the stove.

Recall from Figure 6 that although T_f , T_b , and T_w can be respectively set to 860K, 650K, and 373.15K, there are still six unknown temperatures: T_n , T_a , T_{an} , T_e , T_{p1} , and T_{p2} . In order to eliminate unnecessary variables, we remember that the temperature within a control volume is defined as the average of the inlet and outlet temperatures of that volume, shown in Equations 44 and 45.

$$T_n = \frac{T_{an} + T_f}{2} \quad (\text{Eq. 44})$$

$$T_a = \frac{T_{an} + T_e}{2} \quad (\text{Eq. 45})$$

This eliminates T_n and T_a , leaving only four unknown temperatures. Next, an energy balance may be written for the nozzle control volume at temperature T_n . The energy lost from convective heat transfer, $q_{conv,s}$, results in a temperature drop from the fluid. A similar expression is presented by Kausley[7]. This is shown below in Equation 46.

$$\dot{m} \int_{T_{an}}^{T_f} C_p(T) dT = q_{conv,s} = h_s A_s \left(\frac{T_{an} + T_f}{2} - T_{p1} \right) \quad (\text{Eq. 46})$$

A similar energy balance, Equation 47, may be written for the temperature drop that results from convective heat transfer to the sides of the pot.

$$\dot{m} \int_{T_e}^{T_{an}} C_p(T) dT = q_{conv,a} = h_a A_{ps} \left(\frac{T_{an} + T_e}{2} - T_{p2} \right) \quad (\text{Eq. 47})$$

Next, an energy balance is written for the bottom of the pot. Because steady state conditions are assumed, the pot bottom temperature, T_{p1} , does not vary. As a result, heat transfer to the pot bottom must be equal to heat transfer from the pot bottom. This is shown in Equations 48 and 49.

$$q_{conv,p1} = q_{rad,bp} + q_{conv,s} \quad (\text{Eq. 48})$$

$$h_w A_s (T_{p1} - T_w) = \sigma \varepsilon_b F_{bp} A_b (T_b^4 - T_{p1}^4) + h_s A_s \left(\frac{T_{an} + T_f}{2} - T_{p1} \right) \quad (\text{Eq. 49})$$

Finally, a similar energy balance can be written for the sides of the pot, as shown in Equations 50 and 51. It should be realized that heat transfer to the pot side must be equal to heat transfer from the pot side.

$$q_{conv,p2} = q_{conv,a} \quad (\text{Eq. 50})$$

$$h_w A_{ps} (T_{p2} - T_w) = h_a A_{ps} \left(\frac{T_{an} + T_e}{2} - T_{p2} \right) \quad (\text{Eq. 51})$$

These four equations create a nonlinear system of equations that have only four unknowns. It can be solved by Newton-Raphson method. The method used to solve these equations is detailed in the optimization section of this report.

Stove Efficiency

It is possible to solve for all the geometries, fluid flow conditions, heat transfer rates, and temperatures for a variety of temperatures and still not know the optimum stove. Remember, the primary consideration of stove design is to maximize efficiency so that meals may be cooked with the lowest possible use of fuel. This both reduces time spent gathering fuel, as well as the overall amount of emissions released during the cooking process. This also means that we must come up for an expression for efficiency. Efficiency is commonly defined as the ratio of useful work over the total amount of work done. In the case of a cook stove, that can be translated to be the total heat transfer to the pot's contents over the total amount of energy released.

Employing the same assumptions that have been made throughout this analysis, the total heat transfer to the pot can be described by Equation 52.

$$q_{tot} = q_{rad} + q_{conv,s} + q_{conv,ps} \quad (\text{Eq. 52})$$

Also, the total amount of energy released from the combustion chamber is equal to the total amount of radiation from the bed plus the energy needed to heat ambient air to the flame temperature. This relationship is shown below in Equation 53.

$$Q = \frac{q_{rad}}{F_{bp}} + \dot{m} \int_{T_\infty}^{T_f} C_p(T) dT \quad (\text{Eq. 53})$$

Finally, an expression for efficiency of the stove can be obtained.

$$\eta = \frac{q_{tot}}{Q} = \frac{q_{rad} + q_{conv,s} + q_{conv,ps}}{\frac{q_{rad}}{F_{bp}} + \dot{m} \int_{T_\infty}^{T_f} C_p(T) dT} \quad (\text{Eq. 54})$$

Objective Equation

As noted in earlier sections of this report, because cost and emissions can be best manipulated using qualitative methods, only the efficiency of the stove is effectively evaluated

in a quantitative way. Therefore, the stove efficiency should be maximized. This yields the objective shown below as Equation 55.

$$y = \eta = \frac{q_{rad} + q_{conv,s} + q_{conv,ps}}{\frac{q_{rad}}{F_{bp}} + \dot{m} \int_{T_{\infty}}^{T_f} C_p(T) dT} \quad (\text{Eq. 55})$$

where y is to be maximized. Because η is an efficiency, it should always be between zero and one. Any other solution will indicate an error in some step of the process.

Constraint Equations

Constrain Equations for this optimization problem consists of all the equations, relationships, and limitations discussed previously in the modeling section of this report. These include but are not limited to constraints on the following:

1. Conservation of energy
2. Conservation of mass
3. Geometric relationships
4. Limitations on Temperature
5. Limitations on dimensions

OPTIMIZATION

Introduction

As detailed in previous sections, the simulation of an improved cook stove involved a number of tightly coupled thermodynamic and heat transfer processes. For instance, the temperatures at various points in the stove greatly affected the fluid properties of the air medium transporting heat energy. The approach used to deal with this complexity was based on the Newton-Raphson method.

The simulation began with an initial guess for temperatures at key points in the stove. These temperatures were used to calculate relevant fluid mechanics properties such as density and heat transfer coefficients. Using these calculated values, it was possible to set up control volume energy balances for different regions of the stove. These control volume energy balances were used to calculate the error term for the Newton-Raphson method. Using MATLAB's built-in solving functions, temperatures that satisfied the control volume energy balances were found. It was prohibitively computationally expensive to exhaustively search the solution space for a global optimum of gap size, pot height, pot diameter, and gap width. Also, the method of Lagrange multipliers did not fit the formulation of the problem. Instead, a study of the effect of varying various geometric parameters was performed, and a candidate design for a stove was constructed using insight gained from this process.

For reference to the equations and implementation of the numerous mathematical models, input and output variables, and optimization methods utilized, please see the MATLAB code provided in Appendix G.

Parametric Analysis

The first study of stove parameters performed was a coarse search of the solution space varying the nozzle diameter, gap size, pot height, and pot diameter. The results of this study are presented in Figure 7.

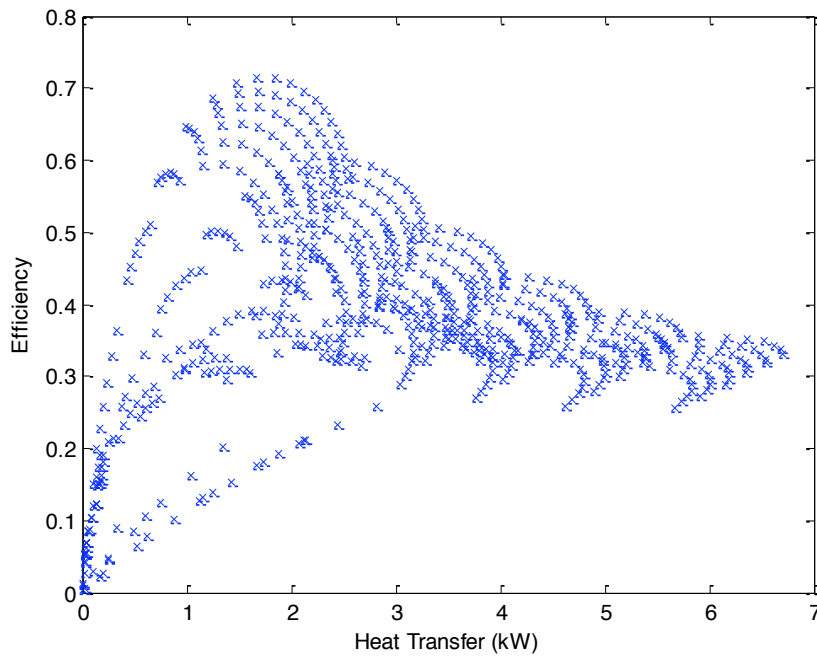


Figure 7. Coarse Search Results

There appeared to be candidate stove designs for any combination of desired heat transfer and efficiency. It turned out that the height of the stove should always be set at its maximum value of 40 cm. This is shown by Figure 8, where stoves with a height of 40 cm are circled in red.

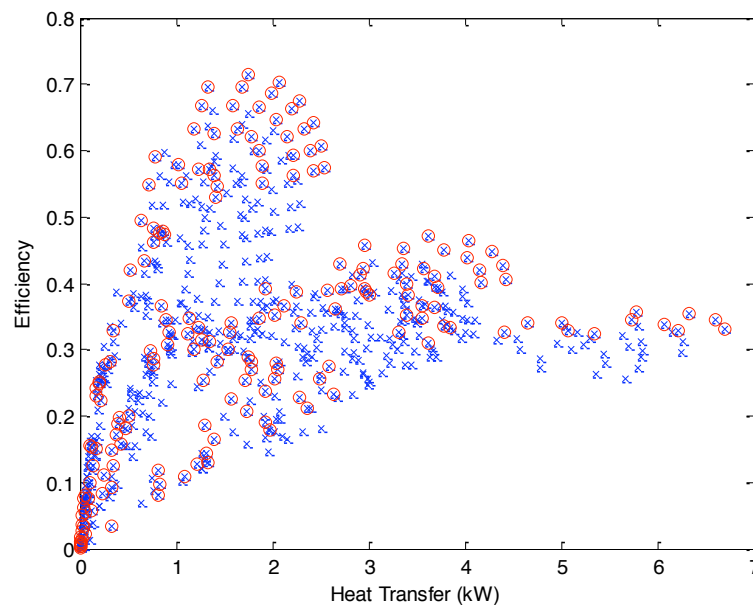


Figure 8. Candidate Stove Designs of Maximum Stove Height

Another parameter that could be set to its upper bound was the nozzle diameter. Figure 9 and Figure 10 show the results simulating the performance of a stove at a fixed diameter of 20

cm and a fixed height of 40 cm. Notice that the optimal efficiency and heat transfer occurred at the maximum nozzle diameter.

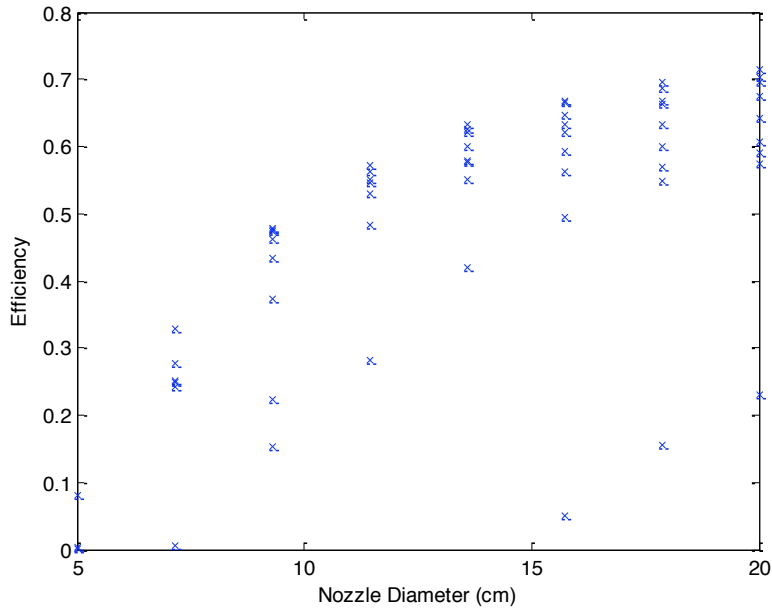


Figure 9. Efficiency of Fixed Dimension Stove

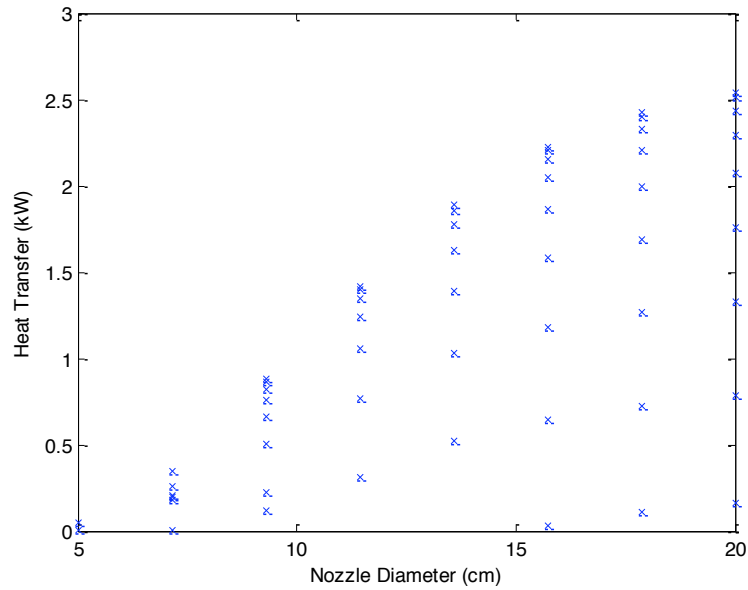


Figure 10. Heat Transfer of Fixed Dimension Stove

Based on the previous two results, it was possible to explore a narrower subset of the solution space more exhaustively. Stove diameter was varied from 20cm to 40cm, and more data points were considered for the gap size.

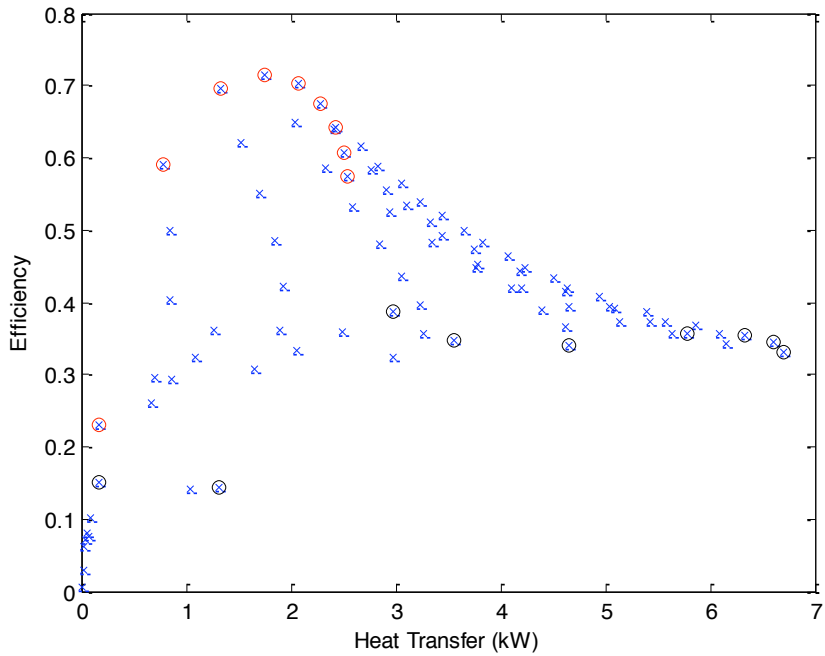


Figure 11. Optimized Stove Design Candidates

The stove configurations circled in red within Figure 11 were for a diameter of 20 cm, and the stove configurations circled in black were a diameter of 40 cm. The stove that displayed the maximum efficiency in the above plot delivered enough power for a family’s cooking needs. Therefore, the optimal stove geometry for our design problem was selected and is presented in Table 5 below.

Table 5. Optimized Stove Geometry and Outputs

Geometry	Value
Gap Size	9.4 mm
Nozzle Diameter	20.0 cm
Stove Diameter	20.0 cm
Stove Height	40.0 cm
Efficiency	0.72
Heat Transfer	1.8 kW

Final Product Drawing

Again, these results indicate that the stove height should be set to its maximum and the stove diameter to its minimum. Furthermore, the nozzle should be set to its maximum diameter, effectively eliminating any of its effects. At these geometries, the ideal gap size is 9.4 m. Figure 12 shows the stove and its dimensions.

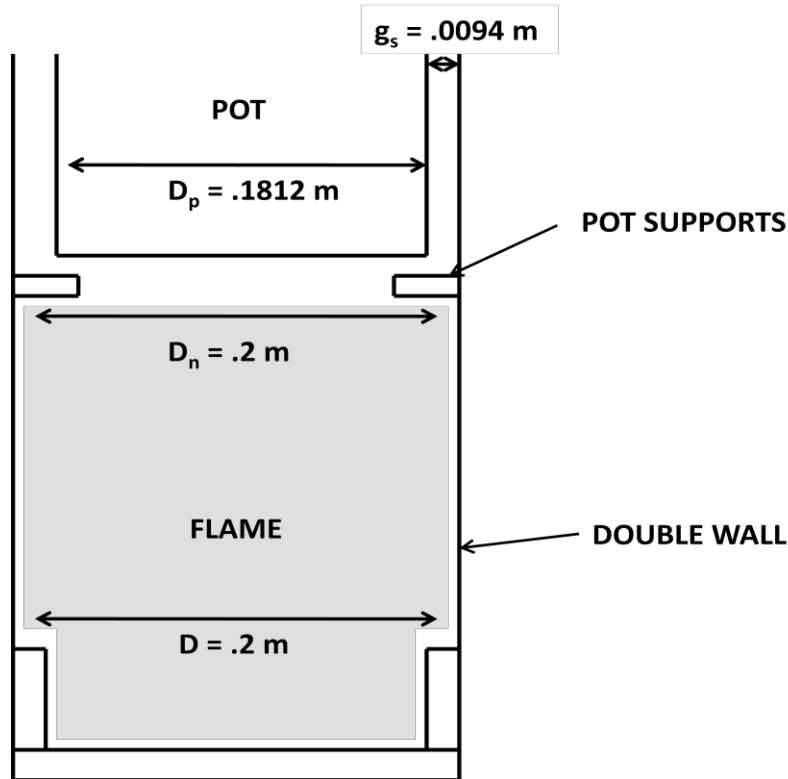


Figure 12. Final Stove and Dimensions

CONCLUSION

From an engineering point of view, the modeling of an improved cook stove undertaken by this team led to a number of insights. It was found that it was possible to capture the heat transfer processes of a stove qualitatively and optimize its geometry. Through analysis, sensitive parameters were isolated. Among the most sensitive for rocket-type stoves with skirts were the gap width and presence of internal features. In fact, the sensitivity of the performance of stoves to internal features caused the potentially innovative design idea of a nozzle to actually decrease stove performance. A final engineering insight was that a high emissivity material inside the stove could greatly improve its performance.

There is still more work that could be done to transform this initial contribution of stove models into a real product. First, testing of human factors, such as how cooks' existing habits impact the real-world performance of the stove, should be undertaken. Also, experiments to establish quantitatively accurate correlations for heat transfer and efficiency numbers could be performed. There were many simplifying models used, and experiments on real rocket stoves could validate or improve their accuracy. Effects that should be considered in more detail include the fuel-air ratio for combustion, the effect of non-adiabatic walls, and the heat transfer coefficient of the liquid in the stove. Despite the modeling challenges, it was possible to design a cook stove for the developing world that exhibited substantial improvements over native technology. Deploying such a technology would improve the quality of life for millions across the globe and significantly contribute to a reduction of emissions of greenhouse gases.

REFERENCES

- [1] Smith, K.A. "Indoor air pollution in developing countries: recommendations for research." *Indoor Air*. 12 (2002): 198-207.
- [2] Achard F, Eva H.D., Stibig H.J., Mayaux P., Gallego J., Richards T., Malingreau J.P., "Determination of deforestation rates of the world's humid tropical forests." *Science*. 297(2002):999-1002.
- [3] Bruce, N., Perez-Padilla, R., Albalak, R. "Indoor air pollution in developing countries: a major environmental and public health challenge." *Bulletin of the World Health Organization*. 78 (2000): 1078-1092.
- [4] Baldwin, Samuel F.. *Biomass Stoves: Engineering Design Development and Dissemination*. New York: Vita Pubns, 1988.
- [5] Still, Dean, Nordica MacCarty. "Cooking with Less Fuel: Breathing Less Smoke." Aprovecho Research Center Library. 2009. Sponsoring Foundations: Aprovecho Research Center, World Food Programme, School Feeding Service (PDPF), Partnership for Clean Indoor Air, Shell Foundation, EPA.
<<http://www.aprovecho.org/lab/pubs/researchlib/category/1/design>>.
- [6] Associated Press. "Cottage Grove company sends 'rocket stoves' to Haiti." 24 Jan. 2010.
<http://www.oregonlive.com/news/index.ssf/2010/01/cottage_grove_company_sends_ro.html>
- [7] Kausley, Shankar B., Aniruddha B. Pandit. Modelling of solid fuel stoves. *Fuel* 89 (2010) 782-791.
- [8] Steward, F.R. *Prediction of Height of Turbulent Diffusion Buoyant Flames*. Combustion Science and Technology, Vol. 2, pp. 203-212, 1970
- [9] Bussmann, Paulus. *Woodstoves: Theory and Applications in developing countries*. Thesis (Ph. D.)--Technische Universiteit Eindhoven, 1988.
- [10] Bergman, Theodore L., David P. Dewitt, Frank P. Incropera, and Adrienne S. Lavine. *Fundamentals of Heat and Mass Transfer*. 6 ed. New York, NY: Wiley, 2006. Print.
- [11] SFPE Handbook of Fire Protection Engineering 2nd Edition.
- [12] Hottel, H., 1954, in *Heat Transmission*, W.H. McAdams (ed.), 3rd edition, McGraw-Hill, New York.
- [13] Dirker, J. and Meyer, J. P. (2005) *Convective Heat Transfer Coefficients in Concentric Annuli*, *Heat Transfer Engineering*, 26: 2, 38 — 44
- [14] *VDI-Wärmeatlas*, 7th edition, Düsseldorf 1994.
- [15] Lytle, D. and Webb, B.W. *Air jet impingement heat transfer at low nozzle-plate spacings*, *International Journal of Heat and Mass Transfer*. Vol. 37, No. 12, pp. 1687-1697, 1994.
- [16] Winiarski, Larry. "Ten Design Principles for Wood Burning Stoves." Aprovecho Research Center Library. 2009. Aprovecho Research Center. <<http://www.aprovecho.org/lab/pubs/researchlib/category/1/design>>.
- [17] Bryden, Mark, Still, Dean, Scott, Peter, Hoffa, Geoff, Ogle, Damon, Bailis, Rob, Goyer, Ken. "Design Principles for Wood Burning Cook Stoves." *Aprovecho Research Center Library*. 2005. Sponsoring Foundations: Aprovecho Research Center, Shell Foundation, EPA.
<<http://www.aprovecho.org/lab/pubs/researchlib/category/1/design>>.
- [18] "Official Home Page of the Best Rocket Stoves on the Planet - Welcome to StoveTec." *Official Home Page of the Best Rocket Stoves on the Planet - Welcome to StoveTec*. N.p., n.d. Web. 29 Jan. 2010. <<http://www.stovetec.net/us/index.php>>.

- [19] Hudelson, Nordica A., Bryden, K.M. and Still, Dean. "Global Modeling and Testing of Rocket Stove Operating Variations." Department of Mechanical Engineering, Iowa State University, Ames, IA 50011-2161.
- [20] An Improved Wood Cookstove: Harnessing Fan Driven Forced Draft for Cleaner Combustion <<http://www.bioenergylists.org/stovesdoc/apro/witt/Final%20Cookstove%20Report%22-%20May05-3.pdf>>.
- [21] Barnes, Douglas F, Openshaw, Keith, Smith, Kirk R, van der Plas, Robert. "The design and diffusion of improved cooking stoves." *The World Bank Research Observer*. Cary: Jul 1993. Vol. 8, Iss.2; pg. 119.
- [22] Smith K.R., Shuhua G., KUN H. and Daxiong Q. "One Hundred Million Improved Cookstoves in China: How Was It Done?" *World Development*, Vol. 21, No. 6, pp. 941-961, 1993.